A Study of a Leaf-Shaped Bowtie Antenna Backed by an Electromagnetic Band Gap Structure

Tomoyuki KOYANAGI Manabu Yamamoto Toshio Nojima

Graduate School of Information Science and Technology, Hokkaido University

Kita 14, Nishi 9, Kita-ku, Sapporo, 060-0814 Japan

E-mail: yamamoto@wtemc.ist.hokudai.ac.jp

1. Introduction

Ultra-wideband (UWB) radio technology has recently attracted considerable attention for various applications, such as short-range high-speed communication, sensor networks, radar and location tracking. As a planar-type wideband antenna being useful for UWB radio systems, the authors have previously proposed a leaf-shaped bowtie antenna [1]. It have been also demonstrated that unidirectional radiation characteristics can be obtained over a wide frequency range by placing the antenna parallel to a reflector [2]. For the case when a perfect electric conductor (PEC) plane is used as the reflector, the antenna height from the reflector is chosen to be one-quarter wavelength of the operating center frequency in order to avoid the degradation of the antenna characteristics [2],[3]. In recent years, it is reported by many researchers that unidirectional beam can be realized by arranging omnidirectional antennas on electromagnetic band gap (EBG) structures with the antenna height of less than one-quarter wavelength [4]-[6]. This paper presents a study on a low profile unidirectional UWB antenna consisting of a leaf-shaped bowtie antenna and a mushroom-type electromagnetic band gap (EBG) reflector [6]. In order to demonstrate effective performance of the proposed configuration, fundamental characteristics of the antenna are investigated and revealed by the finite-difference time domain (FDTD) analysis and measurements.

2. Antenna Structure

Fig. 1 shows the structure of a leaf-shaped bowtie antenna backed by an EBG reflector. Two leaf-shaped radiating elements are arranged on top and bottom surfaces of a dielectric substrate having a thickness of t and a relative permittivity of ε_r. The radiating element is designed by rounding the corner of the square copper sheet with the curvature radius of R_s and the central angle of α. The side length of the square shape is denoted by L_e. The radiating elements are excited by a tapered microstrip line, which act as an impedance transformer and a balun. The antenna substrate is placed parallel to a mushroom-type EBG reflector at a distance of d. As shown in Fig. 2, the EBG reflector is composed of a periodic 9×9 array of square patches printed on a dielectric substrate having the thickness of h. Each patch is connected to a bottom ground plane by using a metal via whose diameter is r. The extent and relative permittivity of the dielectric substrate for the EBG reflector are the same as those of the antenna substrate. The structural parameters assumed in the following investigation are given in Table 1. The parameters of the radiating elements and feeding circuit are optimized for operating in the UWB frequency band (3.1-10.6GHz) when the EBG reflector is not attached [1].

3. Simulated and Measured Results

Fig. 3 shows the frequency dependence of the reflection phase of normally incident plane wave on the mushroom-type EBG structure having the geometrical parameters given in Table. 1. The results are calculated by using the formula reported in [5]. The zero degree reflection phase is observed at 8.2GHz. At this frequency, the EBG structure acts as a perfect magnetic conductor (PMC) surface [6].

The performances of the leaf-shaped antenna backed by the EBG reflector are evaluated by the FDTD analysis and measurements. The spacing between the antenna substrate and the EBG reflector is chosen to be d = 2mm = 0.055λ, where λ is the free space wavelength at 8.2GHz. The prototype antenna and EBG reflector are fabricated by using ARLON DiClad 880 dielectric substrate.

Simulated and measured reflection coefficients S_{11} at the input port of the antenna are shown in Fig. 4. For the evaluation of the S_{11}, the reference impedance is assumed to be 50Ω. The measured reflection is less than –10dB over the frequency range from 6.4 to 9.0GHz. On the other hand, the simulated one is larger than –10dB around 7.5 and 9.0GHz. The discrepancy between the measured and simulated results may be attributed to the effect of fabrication error of the prototype antenna.

The co-polarization patterns in the H-plane (*xz*-plane) and E-plane (*yz*-plane) are shown in Fig. 5 and Fig. 6, respectively. As can be seen from the figures, simulated and measured results are in good agreement. Unidirectional radiation characteristics are obtained over the frequency band of 5 to 9GHz. On the other hand, the deterioration of the radiation patterns in both E- and H-planes are observed at 10GHz. Especially, the H-plane pattern contains many lobes and nulls.

In order to investigate the mechanism for the deterioration of the radiation patterns, current distributions on the patches of the EBG reflector are simulated. The simulated current distributions are shown in Fig. 7. At each frequency, the results are normalized by the maximum current amplitude. At the frequency around 8GHz, it can be seen that most of the current concentrate only on the patches underneath the radiating elements. On the other hand, strong currents are induced even on the patches being far from the radiating elements at 10GHz. For this case, unwanted radiation is generated by the patches of the EBG reflector. This results in the degradation of the radiation pattern described above.

Fig. 8 shows the frequency response of the actual gain observed in the z-direction. The simulated result coincides well with measurements. The maximum gain of about 10dBi is obtained at 7.5GHz. Upper and lower frequencies at which the antenna gain degrades by 3dB from the maximum gain are 6GHz and 8.7GHz, respectively. It is found from Fig. 3 that the reflection phase of the EBG at these frequencies are 135 and –45 degrees, respectively. These results imply that the –3dB gain bandwidth can be estimated by finding the frequency region of the reflection phase in the range of $90^\circ \pm 45^\circ$.

4. Conclusions

A leaf-shaped bowtie antenna backed by a mushroom-type EBG reflector has been presented in this paper. Fundamental characteristics of the antenna have been evaluated by the finite-difference time domain (FDTD) analysis and measurements. It is confirmed that low-profile unidirectional antenna having wideband characteristics can be realized by placing the leaf-shaped bowtie antenna parallel to the EBG reflector at a distance of less than one-quarter wavelength. The maximum gain of about 10dBi is obtained around the frequency at which the zero degree reflection phase of EBG occurs.

References

[1] M. Ameya, M. Yamamoto, and T. Nojima, “An omnidirectional UWB printed dipole antenna with small waveform distortion,” Proc. of Progress In Electromagnetics Research Symposium 2006, 4P3, p.515, Aug. 2006.

[2] M. Ameya, M. Yamamoto, T. Nojima, and K. Itoh, “Leaf-shaped Element Bowtie Antenna with Flat Reflector for UWB Applications,” IEICE Trans. Commun., vol.E90-B, no.9, pp.2230-2238, Sept. 2007.

[3] M. Ameya, Y. Ito, M. Yamamoto, and T. Nojima, “Experimental study on 2-element UWB array antenna using leaf-shaped bowtie element,” Proc. of 2007 International Symposium on Antennas and Propagation, 2A4-1, Aug. 2007.

[4] F. Y. Yang and Y. Rahmat-Samii, “Reflection phase characterizations of the EBG ground plane for low profile wire antenna applications,” IEEE Trans. Antennas Propag., vol.51, no.10, pp.2691-2703, Oct. 2003.

[5] M. Z. Azad and M. Ali, “Novel wideband directional dipole antenna on a mushroom like EBG structure,” IEEE Trans. Antennas Propag., vol. 56, no. 5, pp.1242-1250, May 2008.

[6] Y. Rahmat-Samii and H. Rajagopalan, “From a PEC ground plane to an EBG surface: Understanding the underlying physics,” Proc. of ISAP2009, pp. 285-288, Oct. 2009.

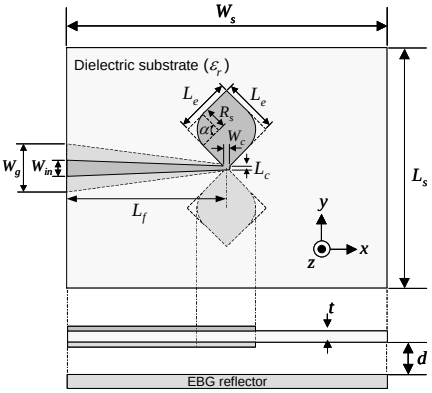

Fig. 1 Antenna structure.

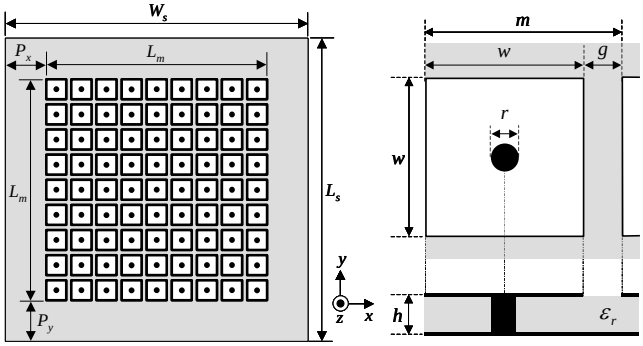

Fig. 2 Geometry of an EBG reflector.

Table 1 Structural parameters.

W_s [mm]	L_s [mm]	t [mm]	d [mm]	ε_r
100	100	0.762	2.0	2.17

L_f [mm]	L_c [mm]	W_c [mm]	w[mm]	g[mm]
50.0	0.2	0.2	7.5	1.0

L_e [mm]	α[deg]	R_s [mm]	W_{in} [mm]	W_g [mm]
12.0	90	7.1	2.4	12.0

r [mm]	h [mm]	P_x [mm]	P_y [mm]	L_m [mm]
0.8	1.575	12.25	12.25	75.5

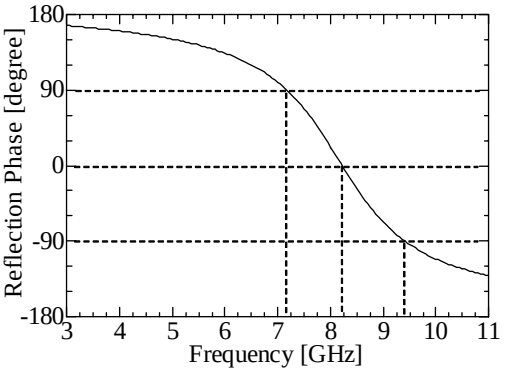

Fig. 3 Reflection phase of EBG reflector.

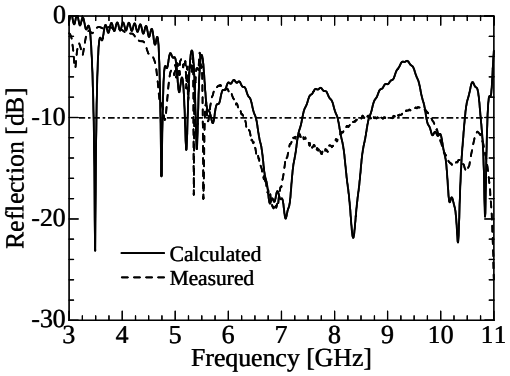

Fig. 4 Reflection coefficient S_{11} vs. frequency.

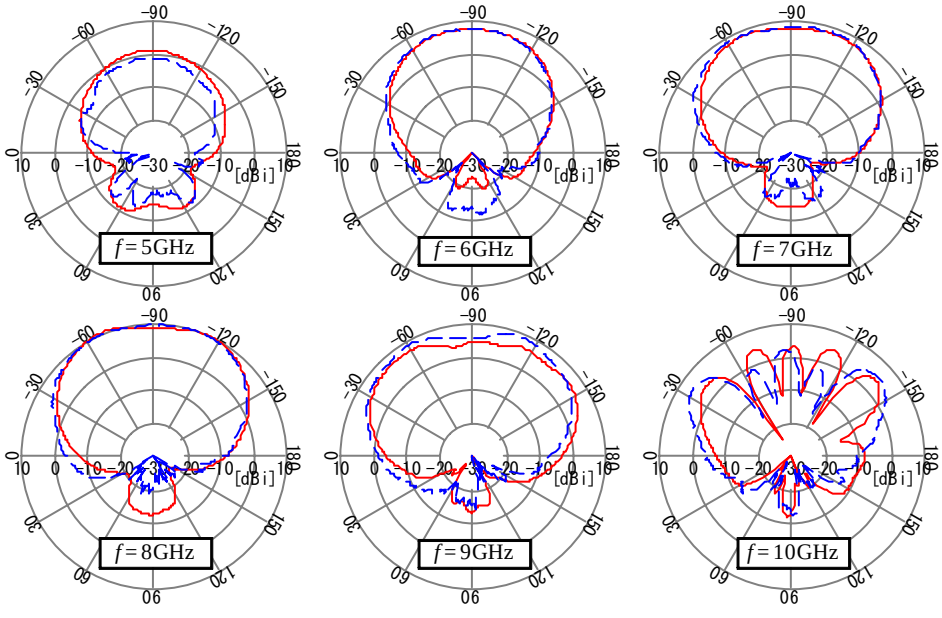

Fig. 5 Radiation patterns in *xz*-plane (co-polarization).

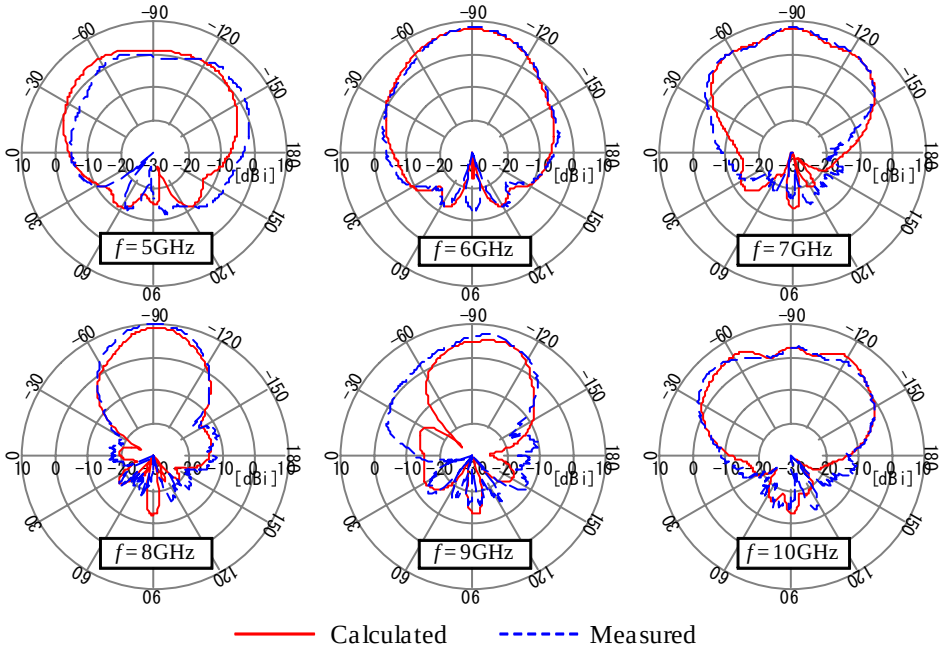

Fig. 6 Radiation patterns in *yz*-plane (co-polarization).

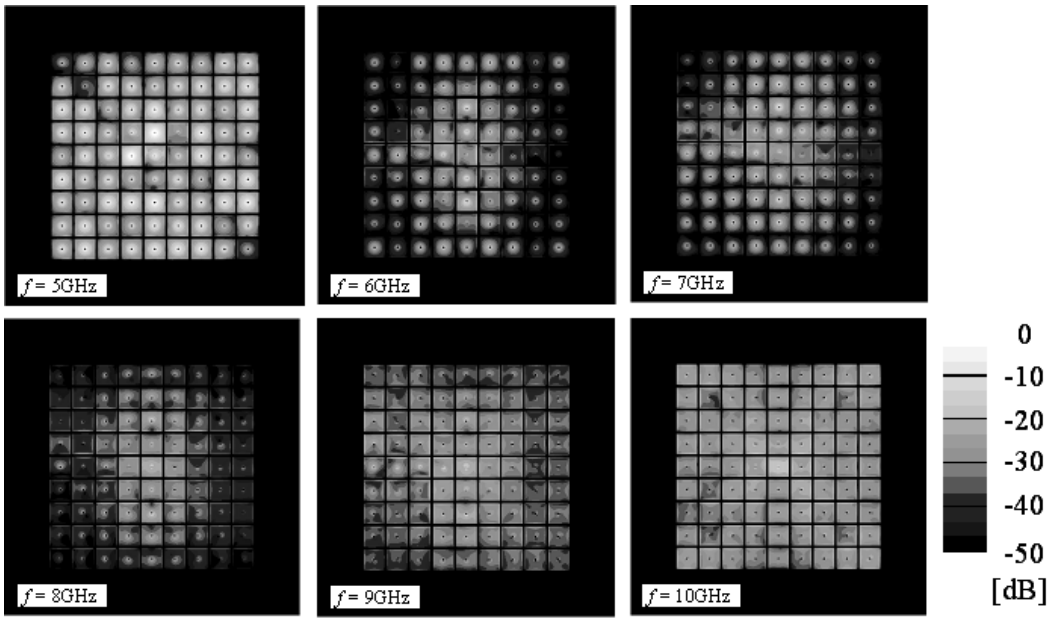

Fig. 7 Current distributions on EBG reflector.

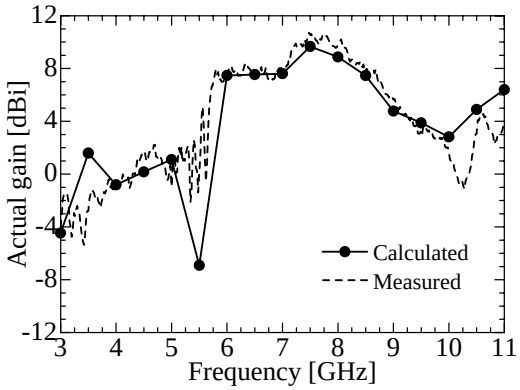

Fig. 8 Frequency response of actual gain observed in z-direction.